ESD-TR-77-173

Technical Note

1977-30

J. R. Vernau

An Attitude Control System for a Large Geosynchronous Earth-Pointing Satellite

5 July 1977

Prepared for the Department of the Air Force
under Electronic Systems Division Contract F19628-76-C-0002 by

Lincoln Laboratory
MASSACHUSETTS INSTITUTE OF TECHNOLOGY
LEXINGTON, MASSACHUSETTS

The work reported in this document was performed at Lincoln Laboratory, a center for research operated by Massachusetts Institute of Technology, with the support of the Department of the Air Force under Contract F19628-76-C-0002.

This technical report has been reviewed and is approved for publication.

FOR THE COMMANDER

Raymond L. Loiselle, Lt. Col., USAF
Chief, ESD Lincoln Laboratory Project Office

MASSACHUSETTS INSTITUTE OF TECHNOLOGY
LINCOLN LABORATORY

AN ATTITUDE CONTROL SYSTEM FOR A LARGE GEOSYNCHRONOUS EARTH-POINTING SATELLITE

J. R. VERNAU
Group 68

TECHNICAL NOTE 1977-30

5 JULY 1977

LEXINGTON MASSACHUSETTS

ABSTRACT

The proposed attitude control system addresses three major problem areas:

(1) Operation within a high torque environment.

(2) The preservation of vehicle attitude in the event that the optical attitude sensors are destroyed by external means.

(3) Longevity, the need for the vehicle to remain operational for periods in excess of seven years.

It is shown that for a given momentum wheel capacity, orthogonal triad torquing will allow greater growth in the disturbance torque environment than a biased momentum system. Orthogonal triad torquing is therefore to be preferred for a general purpose platform where the external geometry of the vehicle is variable.

Primary attitude sensing is accomplished by IR earth sensors for pitch and roll, and processed sun elevation information for yaw. The normal operating mode uses these sensors to update a redundant inertial unit made up of six SDF gyros, automatic update algorithms are suggested designed to prevent a malfunctioning optical sensor from de-erecting the inertial system.

In the event that the inertial system suffers total failure, a backup mode allows the optical sensors to feed the control system directly. The inability of the sun elevation sensor to provide yaw information for short periods centered on local midnight and midday means that the yaw channel must operate in an open loop mode during these periods. A small pitch momentum together with a compensating roll-yaw torque couple is used to stiffen the yaw axis during these 'coast' periods.

TABLE OF CONTENTS

AN ATTITUDE CONTROL SYSTEM FOR A LARGE GEOSYNCHRONOUS EARTH-POINTING SATELLITE

1. DISCUSSION

The term large in this instance refers to a satellite in the 2000 to 3000 lb. class, with external body torque in excess of 50 micro-ft.-lbs. Two of the major issues to be considered when outlining an attitude control system of this type are torquing methods and attitude sensing. In the case of torquing methods the control system may be classified by the method employed to control the attitude of the body fixed roll-yaw plane. If the system relies upon a relatively large bias momentum to resist external torques, then the system, not surprisingly, is categorized as a "biased momentum" system. If orthogonal triad attitude sensing and body torquing is employed, such that the system does not rely upon a large resident momentum, then the system may be categorized as "momentumless".

Biased momentum systems are, in general, somewhat simpler in that correctional torques need be produced about two axes only. Also, direct yaw sensing is not necessary. However, biased momentum systems become a little unwieldy in terms of bias requirement in a high torque environment. For example, if we assume the simplest case where the momentum bias vector is normal to the orbit plane, and forms a constant angle with the body fixed axes (i.e., rigidly mounted) then it is quite straightforward to calculate the required bias.

$$T_{\sin} \omega_o t = h_1 \dot{E}_3 + h_1 \omega_o E_2 \tag{1}$$

$$T_{\cos} \omega_o t = -h_1 \dot{E}_2 + h_1 \omega_o E_3 \tag{2}$$

h_1 = pitch bias momentum

$$\therefore h_1(\text{requ}) = \frac{T}{E_2} \cdot t \cdot \cos \omega_o t \tag{3}$$

Let $E_{2(PK)} = 0.1°$

Let $T = 40 \times 10^{-6}$ ft-lbs.

$$h_{1(\text{Pk. Requ.})} = \frac{T}{E_2} \cdot \frac{2\pi}{\omega_o} = 1980 \text{ ft-lb-secs.} \tag{4}$$

The peak level and the assumed form for the torques are appropriate for a vehicle such as ATS-F. If the bias vector were gimballed, so decoupling the roll and yaw errors, then yaw pointing becomes our criterion and some relaxation may be possible. In fact, the required bias is a linear ratio of permitted roll to yaw error. If a yaw error of 0.6° were permitted then the bias requirements would reduce to 330 ft-lb-secs.

Both of these methods rely upon the bias momentum being very large compared to the accumulated momentum for any single orbit, such that the vector sum produces an acceptably small error angle. Consequently, having chosen a given bias, any further increase in the torque environment is paid for directly in reduced pointing accuracy, or increased fuel consumption.

In the case of the rigidly mounted wheel the required bias is pushing the frontiers of technology, consequently reliability data is minimal to non-existent.

In the case of the gimballed wheel the bias is less breathtaking but still forty times greater than LES-8/9, and we have the added complication of the gimbal mechanism, whether it is a second wheel or a true gimbal.

The "momentumless" system on the other hand requires that correctional torques be available about all three axes. Furthermore, attitude sensing is required for all three axes, whereas the bias system requires attitude sensing about two axes only. However, the volatile momentum storage requirements are considerably less for the "momentumless" system. This is because the storage capacity need only equal the peak momentum accumulations for any orbit. It is quite straightforward to calculate the required storage capacity for a "momentumless" system assuming the same torque environment as above.

Assuming an idealized controller and zero pointing errors,

$$T \cdot \sin \omega_o t = h_2 - h_3\omega_o \tag{5}$$

$$T_{\cos} \omega_o t = h_3 + h_2\omega_o \quad (6)$$

h_2, h_3 = roll and yaw wheel momentum respectively

$$h_2(t) = T \cdot t \cdot \sin \omega_o t \quad (7)$$

$$h_2(pk) = 3\pi T/2\omega_o = 2.6 \text{ ft-lb-secs.} \quad (8)$$

$$h_3(t) = T \cdot t \cdot \cos \omega_o t \quad (9)$$

$$h_3(pk) = 3.46 \text{ ft-lb-secs.} \quad (10)$$

The assumed torque would in practice contain several harmonics plus a DC term, particularly during the solstice. However, this is not an attempt to calculate the actual requirements of a satellite, but simply to compare the momentum storage needs of two different classes of control system when exposed to the same torque environment. It is clear that the momentumless configuration requires much less storage capacity than either of the biased systems, and furthermore the attitude errors in all three axes can be zero, whereas this is not possible with the biased systems. The price paid for this is the need for three axis torquing and attitude sensing. The point to be considered in this particular discussion is the uncertainty of the torque environment.

We are considering a control system suitable for a general-purpose vehicle, hence the body geometry and therefore the torques must be considered as unknown. If the body torques increased by an order of magnitude above those figures mentioned, then the biased systems would be totally unfeasible with present technology, whereas the storage requirements of the momentumless system would remain relatively modest (< 30 ft-lb-secs) and well inside the proven capabilities of the industry.

In general, the momentumless system configuration will permit operation within the maximum torque environment for a given storage capability. The small increase in complexity brought about by the necessity for one more

torquer, plus a small amount of processing in order to derive yaw attitude, is a small price to pay for an optimal system configuration.

1.1 Body Torquers

In order to provide both adequate redundancy and margin for growth in the torque environment, a configuration of four 10 ft-lb-sec. reaction wheels is proposed. The wheels will be symmetrically configured about the three principal axes of the vehicle, such that any wheel provides components of torque and momentum about all three axes. Any three wheels will be able to fulfill the three axes torquing requirement of the momentumless system. The fourth wheel will be unpowered, unless a failure occurs in one of the active wheels. The configuration is shown in Fig. 1.

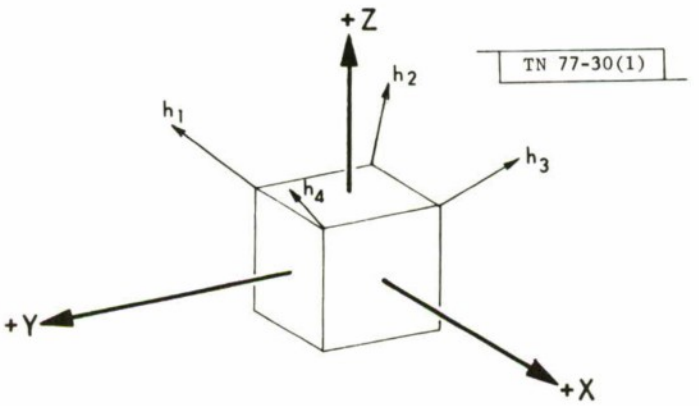

Fig. 1. Reaction wheel momentum vectors.

XYZ represent the vehicle principal axes. h_j represent the torquing axes of the momentum wheel.

If each torquer can provide equal effort, then:

$$h_{(xyz)} = \frac{h_j}{\sqrt{3}} \tag{11}$$

$$\phi = \cos^{-1}\left[\frac{h_{(xyz)}}{h_j}\right] = \frac{1}{\sqrt{3}} = 54.74^\circ \tag{12}$$

Where ϕ represents the angle made by the wheel spin axis with respect to the body fixed principal axes of the vehicle.

If we assume the right-hand rule sign convention, then the momentum matrix would be:

$$\begin{bmatrix} Z \\ X \\ Y \end{bmatrix} = \frac{1}{\sqrt{3}} \begin{bmatrix} +1 & +1 & +1 & +1 \\ -1 & -1 & +1 & +1 \\ +1 & -1 & -1 & +1 \end{bmatrix} \begin{bmatrix} h_1 \\ h_2 \\ h_3 \\ h_4 \end{bmatrix} \tag{13}$$

In order to determine net momentum about any principal axis the individual wheel momentums are measured and simply plugged in. Inspection of the above matrix reveals the torquing rules, which are tabulated below.

MISSING WHEEL	+Z	+X	+Y
h_4	$+h_1^* + h_3^*$	$-h_2^* + h_3^*$	$+h_1^* - h_2^*$
h_3	$+h_2^* + h_4^*$	$-h_1^* + h_4^*$	$+h_1^* - h_2^*$
h_2	$+h_1^* + h_3^*$	$-h_1^* + h_4^*$	$-h_3^* + h_4^*$
h_1	$+h_2^* + h_4^*$	$-h_2^* + h_3^*$	$-h_3^* + h_4^*$

$\times \frac{1}{\sqrt{3}}$

Thus, this configuration is very simple to use and provides very significant redundancy, in that any wheel may fail without degrading performance in any way.

A further point is that the Draper Laboratory TCP treatment of ball bearings appears to have solved the touchdown problem, so removing reliability based objections to reaction wheels. On the other hand, it seems clear that reaction wheels would be very much more efficient in terms of power usage.

1.2 Attitude Sensing

The decision to employ the momentumless configuration discussed in 1.0 implies the need for yaw sensing.

There are several methods of doing this. With an equatorial orbit a strap-down star tracker viewing Polaris would appear to be a straightforward approach, as used on ATS-F. However, there is no star tracker presently available which shows any indication of possessing the reliability potential which would justify its use on a 7 to 10 year mission. ATS-F is a case in point. Solid State star transit sensors, on the other hand, appear to be relatively simple, and inherently rugged. There are, however, several objections to their use. Heretofor they have been used at high transit rates (such as on the DMS) if the same sensor were used at the body rates appropriate for a stabilized geosynchronous satellite, the signal-noise ratio would be marginal. Possibly this is surmountable, but earth rate star transit sensors are not presently available. Furthermore, an on-board star map would be required, together with an inertial memory to provide attitude data between star updates. None of these objections are very serious, but there seems little point in pursuing a discontinuous system based on a star transit sensor when the sun is readily available together with well developed sun elevation sensors able to provide virtually continuous data. It is proposed therefore that a 360° sun elevation sensor be used to provide yaw sensing, and IR earth sensors similar to the well proven TRW scanning type used to provide pitch and roll. Provided that the orbit is known, yaw information may be derived from the sun elevation sensor over a large part of the orbit. The two periods when yaw derivation is not possible occur at local midnight and midday. The former, because of sun obscuration, the latter due to kinemetic reasons, both periods are of approximately 1 hour in duration. It should be possible then to provide three axis attitude information to the control system directly from the body sensors once the orbit fit data is transmitted to the satellite. This system is analyzed later in this note (Section 2.0, Backup Mode). However, while the "backup mode" is able to fulfill the mission in terms of dynamic performance, it suffers from several disadvantages. The first and major

disadvantage is that the optical sensors are subject to damage through enemy action, either ground based or via killer satellite. If this occurred the vehicle would lose orientation in a very short time.

Furthermore, while the pitch and roll IR sensors are separate, mutually redundant items referenced to the earth, the yaw sensor has no redundancy, and is referenced to ground derived orbit fit data. What is required is a second yaw sensor, both to provide redundancy and a mutual operational check.

Gyroscopes overcome both of these disadvantages. A gyro triad updated from the three axis body sensor would provide sufficient inertial memory to preserve satellite attitude within acceptable limits for several months following an optical sensor wipeout. In the event that the sun elevation sensor failed, or a gross operational check was required, the gyros could be reconnected by ground command into the gyro-compassing mode. This mode has the advantage that it is self erecting, and does not require orbital data. Both of these gyro based systems are discussed in greater detail in Section 3.0.

As an overview, it is proposed that the normal operational system derive attitude data from a rate gyro triad. The gyros will be erected and updated as required by a three axis body sensor which will consist of IR earth sensors for pitch and roll and a sun elevation sensor plus microprocessor for yaw. As an almost equal performance alternate to this configuration the gyros and earth sensors may be connected as an orbital gyrocompass.

In the event that the gyro system suffers catastrophic failure, the control system may enter the "backup mode", in which the optical sensors bypass the gyros and supply the control loop directly.

2. BACKUP MODE

The "backup system" is intended to become operational in the mathematically unlikely event that the gyro package suffers total failure. If this occurs, the pitch, roll and yaw body sensor outputs will bypass the gyro package and feed the control system directly. However, the yaw sensor, as mentioned previously, cannot operate throughout the orbit. For approximately one hour centered on local midnight the sun is obscured. Also, if the sun elevation

angle is zero, then yaw cannot be measured at local midday for kinemetic reasons, even for a non-zero elevation angle the sun elevation sensor becomes progressively less sensitive to yaw motion as local midday is approached. It is proposed then to deactivate the yaw sensor for approximately one hour centered about local midnight and local midday. The satellite will "coast" through these periods with active pitch and roll control only. In order to make the satellite appropriately stiff during these "coast" periods, the "backup mode" will operate with a relatively small momentum vector aligned with the pitch axis. It is interesting to note at this point that in order for the pitch momentum vector to be effective in providing yaw stiffness it is necessary to effect a torque coupling between the roll and yaw axes. In other words, the situation which exists during the coast period is as follows: pitch and roll loops and sensors remain active, the yaw sensor is deactivated, external body torques are occurring naturally about all three axes. If under these circumstances a body fixed momentum vector is aligned with the pitch axis in an attempt to provide yaw stiffness, its effect will be almost totally nullified by the operation of the roll loop. In fact, the body motion about the yaw axis will be governed only by the moment of inertia, with the momentum vector playing no part. This is shown below.

2.1 Equations of Motion For a Zero Momentum Satellite

$$\tau_1 = J_1\ddot{E}_1 + h_3\dot{E}_2 - h_2\omega_o E_3 - h_2\dot{E}_3 - h_2\omega_o E_2 \tag{14}$$

$$\tau_2 = J_2\ddot{E}_2 - (J_2 - J_1 + J_3)\,\omega_o\dot{E}_3 + (J_1 - J_3)\,\omega_o{}^2E_2$$

$$+ h_1\dot{E}_3 + h_1\omega_o E_2 - h_3\dot{E}_1 - h_3\omega_o \tag{15}$$

$$\tau_3 = J_3\ddot{E}_3 + (J_2 - J_1 + J_3)\,\omega_o\dot{E}_2 - (J_2 - J_1)\,\omega_o{}^2E_3$$

$$+h_2\dot{E}_1 + h_2\omega_o - h_1\dot{E}_2 + h_1\omega_o E_3 \tag{16}$$

τ_j = resultant axial torque for j^{th} channel and represents the difference between external disturbance torque and system control torque.

$$\therefore \tau_j = T_{Dj} - \dot{h}_j = T_{Dj} - G_{(j)} \cdot E_j$$

where $G_{(j)}$ represents the gain and shaping, and E_j represents the euler error angle for the j^{th} channel.

h_j = The resultant principal axis angular momentum contained by the reaction wheels.

Equations (15) and (16) are solved below for E_3/T_{D3}, the yaw error angle-yaw disturbance torque transfer function for the coast period, when $G_{(3)} \cdot E_3 = 0$.

Assuming pitch to be effectively decoupled from the roll-yaw plane ($\dot{E}_1 \to 0$).

$$E_3/T_{D3} = \frac{1}{J_3} \cdot \frac{p^2 + \frac{G_{(2)}}{J_2} + \frac{h_1\omega_o}{J_2}}{\left[p^4 + p^2\left(\frac{G_{(2)}}{J_2} + \frac{\omega_o^2 J_2}{J_3} - \frac{h_1\omega_o}{J_3} + \frac{h_1\omega_o}{J_2} + \frac{h_1^2}{J_2J_3}\right) + \frac{G_{(2)}h_1\omega_o}{J_2J_3} + \frac{h_1^2\omega_o^2}{J_2J_3}\right]}$$

P = Laplace Operator

J_j = moment of inertia of the j^{th} axis.

$G_{(2)}$ represents the gain and shaping of the roll channel, and is therefore a design parameter. If we assume typical values for J_2, J_3, and h_1:

$$\frac{G_{(2)}}{J_2} >> \left[\frac{\omega_o J_2}{J_3} - \frac{h_1\omega_o}{J_3} + \frac{h_1\omega_o}{J_2} + \frac{h_1^2}{J_1J_3}\right] .$$

$$\frac{G_{(2)}h_1\omega_o}{J_2J_3} >> \frac{h_1^2\omega_o^2}{J_2J_3}$$

$$E_3/T_{D3} \stackrel{\Omega}{=} \frac{1}{J_3} \cdot \frac{p^2 + \frac{G_{(2)}}{J_2}}{\left[p^4 + p^2\frac{G_{(2)}}{J_2} + \frac{G_{(2)}h_1\omega_o}{J_2J_3}\right]}$$

$$\left[\frac{G_{(2)}}{2J_2}\right]^2 >> \frac{G_{(2)}h_1\omega_o}{J_2J_3}$$

$$E_3/T_{D3} \triangleq \frac{1}{J_3} \cdot \frac{p^2 + \frac{G_{(2)}}{J_2}}{p^4 + p^2 \frac{G_{(2)}}{J_2}} = \frac{1}{J_3 p^2}$$

$$\therefore \quad J_3 \ddot{E}_3 = T_{D3}. \tag{17}$$

This will be recognized as the torque-inertia balance expression for an unrestrained system.

Despite the simplications, it is clear that the pitch axis momentum vector plays very little part in providing stiffness about the yaw axis. Clearly the operation of a 'tight' roll loop is producing torque about the yaw axis, this phenomenon is analyzed in 2.1.1.

2.1.1 Roll-Yaw Compensation

Let us set up the following conditions

(1) Roll loop continuously closed. ($E_2 \triangleq 0$)

(2) Yaw loop open.

(3) Torque applied about the yaw axis at t = 0.

At t = 0 therefore $\dot{E}_3 = E_3 = 0$.

Referring to equations (15) and (16), the roll and yaw equations of motion respectively at t = 0.

$$\tau_2 = J_2 \ddot{E}_2 - h_3 \omega_o$$

$$\tau_3 = J_2 \ddot{E}_3 + J_2 \omega_o \dot{E}_2 + h_2 \omega_o - h_1 \dot{E}_2$$

$$J_3 \ddot{E}_3 = \tau_3 - J_2 \omega_o \dot{E}_2 - h_2 \omega_o + h_1 \dot{E}_2 = \text{total reactive torque.}$$

$$J_3P^2E_3 = \tau_3 - \frac{\omega_o\tau_2}{P} - \frac{\omega_o h_3}{P} - h_2\omega_o + \frac{h_1\tau_2}{J_2P} + \frac{h_1h_3\omega_o}{J_2P}$$

$\tau_3 = T_{D3} - \dot{h}_3 = T_{D3} - T_{3C}$. Where T_{3C} = yaw control torque.

If the total reactive torque about yaw is to be minimized, then the yaw axis must be open loop torqued by T_{3C}:

$$T_{3C} = -h_2\omega_o - \frac{\omega_o\tau_2}{P} \frac{-\omega_o^2 h_3}{P} + \frac{h_1\tau_2}{J_2P} + \frac{h_1h_3\omega_o}{J_2P} .$$

$\tau_2 = T_{D2} - G_{(2)} \cdot E_2$

$$\therefore T_{3C} = \frac{-\omega_o}{P}(T_{D2} - G_{(2)}E_2) - \frac{\omega_o^2 h_3}{P} - h_2\omega_o + \frac{h_1}{J_2P}(T_{D2} - G_{(2)}E_2) + \frac{h_1h_3\omega_o}{J_2P} \quad (18)$$

T_{3C} represents the torque which must be applied to the yaw axis during the coast period in order to minimize the roll-yaw coupling. Notice that two terms are proportional to the integral of net roll axis torque, suggesting the need to know something about the roll disturbance torque during the coast period. The terms in T_{3C} which contain h_3 clearly spring from the momentum cross product term in the roll equation of motion. This would more easily be nulled by torquing the roll axis. The compensating torques for roll and yaw are shown below. They would be calculated on a continuous basis and applied directly to the body torquing mechanism.

Roll Compensation: $-h_1\omega_o E_2 + h_3\omega_o$. (19)

Yaw Compensation: $$-h_2\omega_o - \frac{\omega_o T_{D2}}{P} + \frac{\omega_o G_{(2)}E_2}{P} + \frac{h_1 T_{D2}}{J_2P} - \frac{h_1 G_{(2)}E_2}{J_2P} \quad (20)$$

T_{D2} in (20) above is a measured roll disturbance torque, in order to track it we will designate it T_{D20}.

Inserting these compensation terms into the general equations of motion we obtain:

Let $J_1 = J_3$ for arithmetic convenience.

$$T_{D2} = J_2\ddot{E}_2 - J_2\omega_o\dot{E}_3 + h_1\dot{E}_3 + G_{(2)} \cdot E_2$$

$$T_{D3} = J_3\ddot{E}_3 + J_2\omega_o\dot{E}_2 - (J_2 - J_1)\omega_o^2 E_3 - h_1\dot{E}_2 + h_1\omega_o E_3$$

$$\frac{-\omega_o T_{D20}}{P} + \frac{\omega_o G_{(2)} E_2}{P} + \frac{h_1 T_{D20}}{J_2 P} - \frac{h_1 G_{(2)} E_2}{J_2 P}$$

Making similar assumptions and simplications as before we obtain:

$$E_3/T_{D3}^{(P)} = \frac{1}{J_3} \cdot \frac{1}{P^2 + \frac{h_1^2}{J_2 J_3}} \tag{21}$$

Taking the inverse transform:

$$E_{3(t)} = \frac{T_{D3} \cdot J_2}{h_1^2} \left[1 - \cos\left(h_1/\sqrt{J_2 J_3}\right)t\right] \tag{22}$$

The satellite would therefore nutate at $h_1/\sqrt{J_2 J_3}$ rads/sec. with a peak deviation of $2T_{D3}J_2/h_1^2$ radians.

In this case the pitch momentum vector (h_1) does provide stiffness to yaw body torques, the fact that nutation occurs during the coast period is probably not important providing the excursion is within the system pointing tolerance.

The effect of roll body torque on yaw attitude when the system is thus compensated is shown below:

$$E_{3(P)} = \frac{(T_{D2} - T_{D20})h_1 G_{(2)}}{J_2^2 J_3} \cdot \frac{1}{P\left[(P^2 + \frac{G_{(2)}}{J_2})(P^2 + \frac{h_1^2}{J_2 J_3})\right]}$$

$$E_{3(t)} \underline{\Omega} \frac{h_1(T_{D2} - T_{D20})}{J_3}\left[\frac{t^3}{6J_2} - \frac{t}{G_{(2)}} + \sqrt{\frac{J_2}{G_{(2)}^3}} \cdot \sin\left(\frac{G_{(2)}}{J_2}\right) t\right] \qquad (23)$$

Equation (23) reveals the fact that when compensated in this manner, the yaw axis is somewhat sensitive to the difference between actual roll body torque (T_{D2}) and estimated body torque (T_{D20}). This means that the compensation scheme must be tailored to the disturbance torques which pertain during the coast period. For example, if we consider the body torque forms described by Eqs. (1) and (2), we see that the yaw torque during the midday coast period is quite high and changing rapidly, potentially difficult to predict, the roll torque on the other hand is close to its maximum value and changes very little during the coast period. This is the kind of situation where the form of compensation described by Eq. (19) and (20) would work very well. It would only be necessary to measure h_2 immediately prior to the coast period and plug it into the compensators. The body torques predicted for LES-10 indicate that yaw torque will approach zero, while roll torque will be almost constant. In this situation it would not be appropriate to include all the compensation terms described in Eq. (20), in fact $-h_2\omega_o$ would be the only relevant term, with zero pitch bias.

The required roll-yaw compensation is inestricably coupled to the form and magnitudes of the roll-yaw body torques, the principal axis moments of inertia, together with the actual coasting period. However, available evidence would indicate that providing a measurement of h_2 is taken immediately prior to the coast period, some version of Eqs. (19) and (20) will cover the roll-yaw compensation requirements.

2.1.2. Computer Model

In order to illustrate the foregoing analysis a linearized three axis computer model was constructed on the IBM-370 using an existing numerical integration routine. The system equations of motion are shown below. No particular effort was expended on the loop design other than to assure stability. Apart from the torque compensation terms already discussed, the loop shaping in each case is on integral plus proportional network, feeding a velocity loop to control wheel speed.

$$T_{D1} - \dot{E}_1 K_1 - E_1 B_1 = J_1 \ddot{E}_1 + h_3 \dot{E}_2 - h_2 \omega_o E_3 - h_2 \dot{E}_3 - h_2 \omega_o E_2 \tag{24}$$

$$T_{D2} - \dot{E}_2 K_2 - E_2 B_2 = J_2 \ddot{E}_2 - (J_2 - J_1 + J_3)\omega_o \dot{E}_3 + (J_1 - J_3)\omega_o{}^2 E_2 + h_1 \dot{E}_3 + h_1 \omega_o E_2 - h_3 \dot{E}_1 - h_3 \omega_o \tag{25}$$

$$T_{D3} - \dot{E}_3 K_3 K_4 - E_3 B_3 K_4 = J_3 \ddot{E}_3 + (J_2 - J_1 + J_3)\omega_o \dot{E}_2 - (J_2 - J_1)\omega_o{}^2 E_3 + h_2 \dot{E}_1 + h_2 \omega_o - h_1 \dot{E}_2 + h_1 \omega_o E_3 \tag{26}$$

Pitch Compensation: $+h_2 \omega_o E_2$

Roll Compensation: $-h_1 \omega_o E_2 + h_3 \omega_o$

Yaw Compensation (1): $-h_2 \omega_o$

Yaw Compensation (2): $-\omega_o \int T_{D20}\, dt + \omega_o \int G_{(2)} E_2\, dt + \frac{h_1}{J_2} \int T_{D20}\, dt - \frac{h_1}{J_2} \int G_{(2)} E_2\, dt$

The compensation terms are added to the right side of system Eqs. (24), (25), and (26). The principal moments of inertia are based on mass properties calculation for one version of the projected satellite.

$J_1 = J_2 = J_3 = 2{,}800$ slug - ft^2

$K_1 = K_2 = K_3 = 280$ ft. lbs/radian/sec.

$B_1 = B_2 = B_3 = 28$ ft. lbs/radian

The program listing, appropriately commented, is shown in the Appendix.

Figure 2 illustrates the conclusion that an unaided pitch momentum is unable to provide yaw stiffness in the presence of a tight roll loop.

Figure 3 illustrates the effectiveness of the compensation scheme.

Conditions

Pitch: Loop closed, compensated. $h_1 = 10$ ft-lb-secs. Zero disturbance torque.

Roll: Loop closed, compensated. 50μ-ft-lbs disturbance torque throughout. $h_2^{\cdot} - h_3\omega_o$ measured at coast period inception (11.30 hrs local time).

Yaw: Loop open, compensators (1) and (2). 10μ-ft-lbs disturbance torque throughout.

Figure 4 illustrates the effectiveness of the compensation scheme in the presence of the realistic body torques described by Eqs. (1) and (2).

Conditions (3)

Pitch: Loop closed, compensated, $h_1 = 5$ ft-lb-secs. 50μ-ft-lbs disturbance torque throughout.

Roll: Loop closed, compensated, disturbance torque = $50 \times 10^{-6} \sin \omega_o t$ ft-lbs, $h_2^{\cdot} - h_3\omega_o$ measured at coast period inception (11.30 hrs. local time).

Yaw: Loop open, compensators (1) and (2), disturbance torque = $50 \times 10^{-6} \cos \omega_o t$ ft-lbs.

to = 0600 hrs. local time

Figure 5 shows the effect of the disturbance torques calculated for the current LES-10 configuration. These torques are such that partial yaw compensation is appropriate.

Conditions (1)

Pitch: Loop closed, compensated, disturbance torque = $40 \times 10^{-6} \sin \omega_o t$ ft-lbs. $h_1 = 0$ (initial value)

Roll: Loop closed, compensated, disturbance torque = -12×10^{-6} ft-lbs.

Yaw: Loop open, compensator (1) only. Zero disturbance torque.

Condition (2)

As for condition (1), with all channels uncompensated.

to = 0600 hrs. local time

Coast inception 11.30 hrs. local time

Figure 6 illustrates the major torque inputs for all three channels when fully compensated.

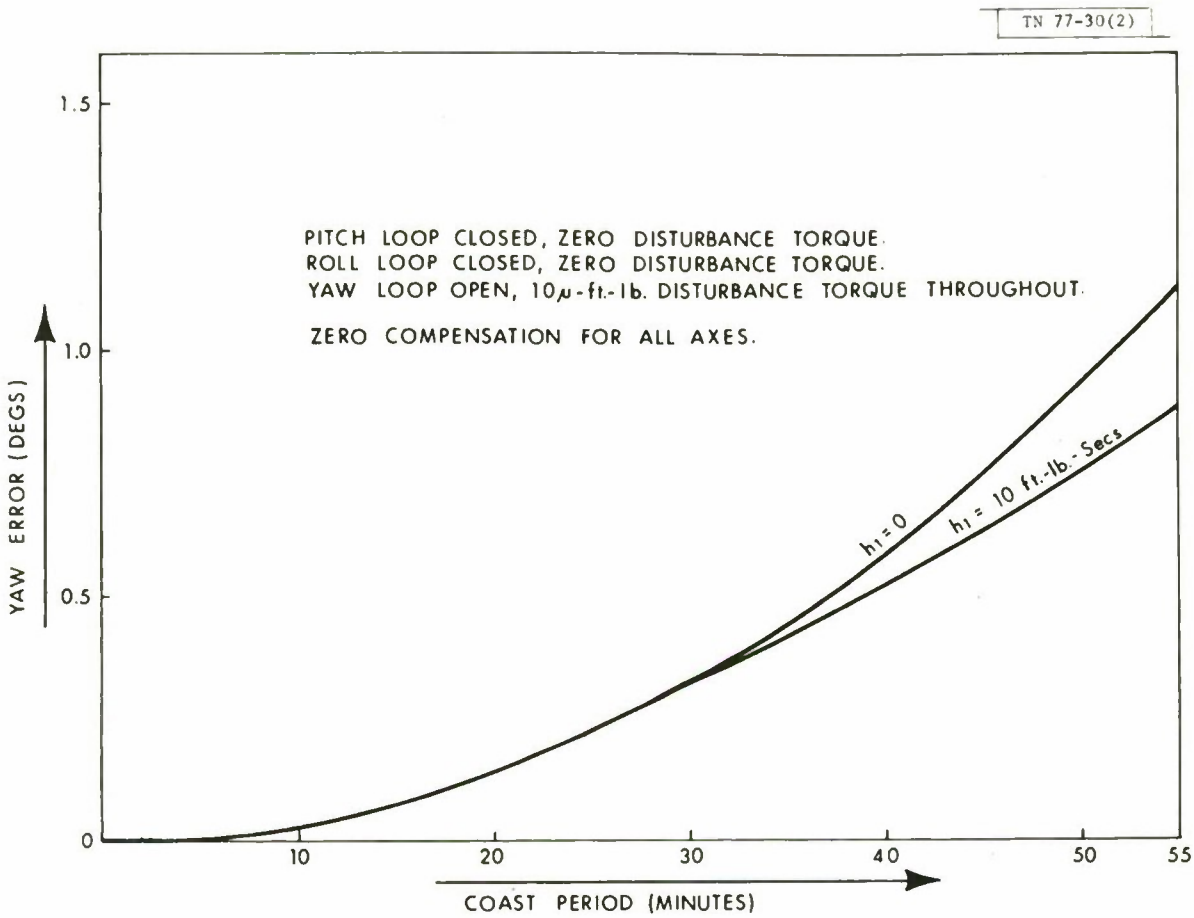

Fig. 2. Uncompensated yaw axis response to a disturbance torque.

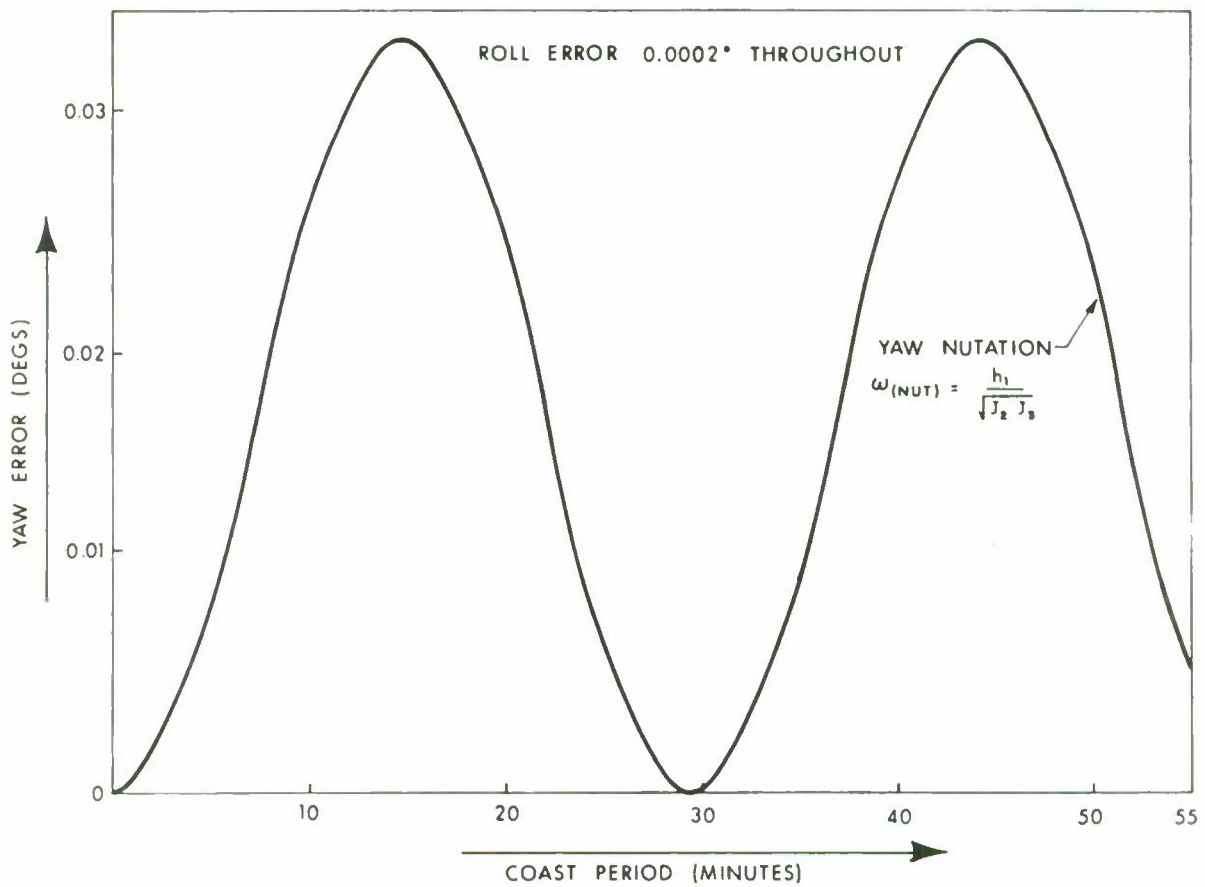

Fig. 3. Fully compensated yaw axis response to a disturbance torque.

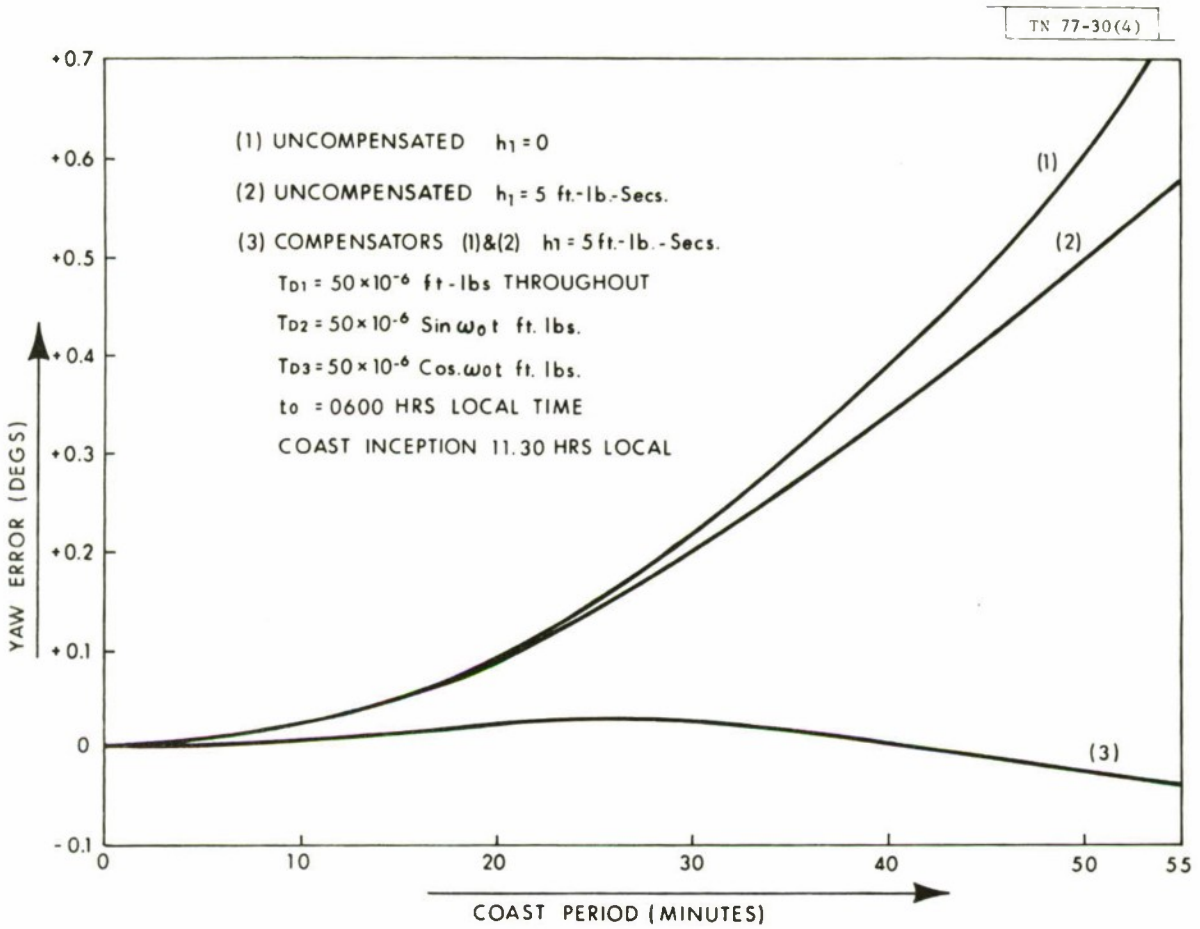

Fig. 4. Comparison of a compensated and uncompensated yaw axis response to typical disturbance torques.

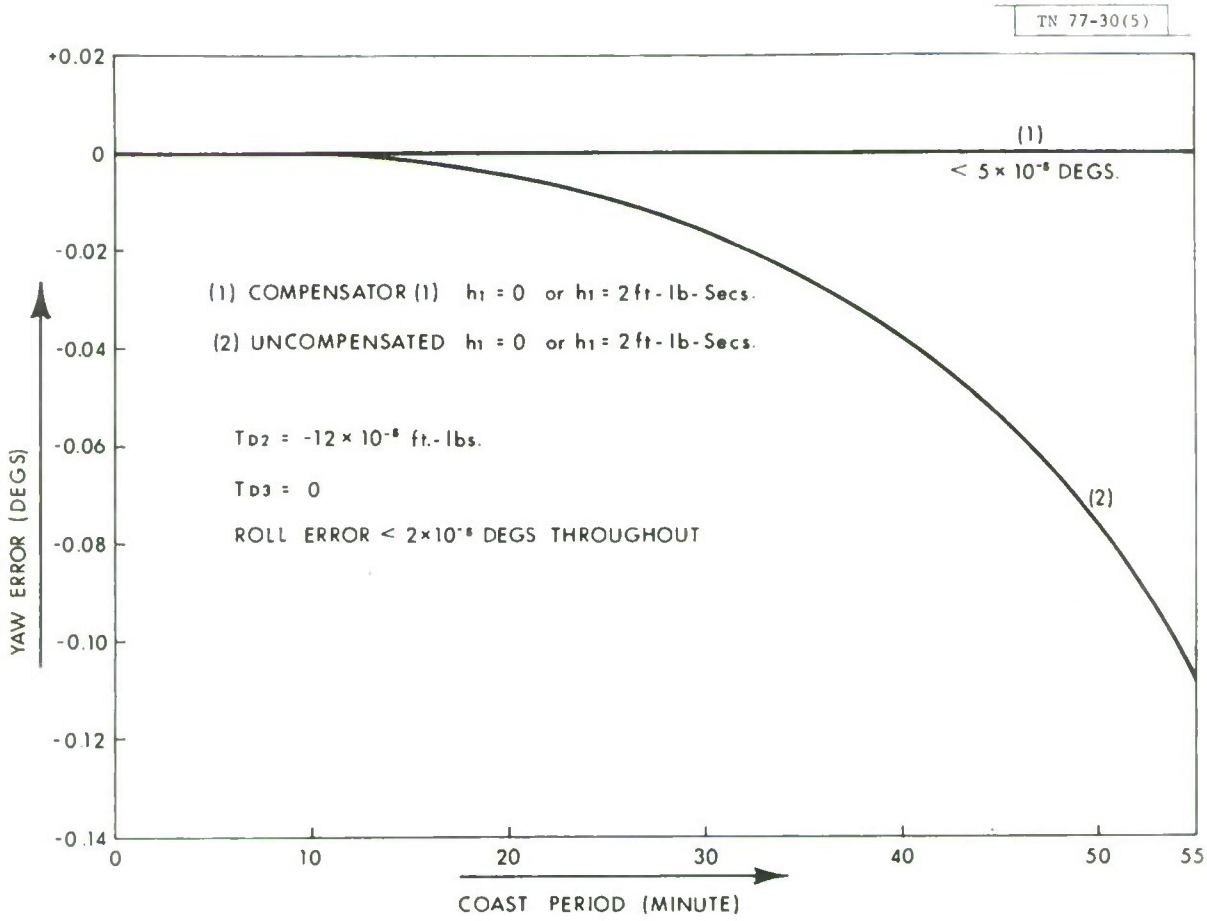

Fig. 5. Comparison of a compensated and uncompensated yaw axis response to a roll disturbance torque.

FULLY COMPENSATED AXIAL TORQUES DURING THE COAST PERIOD

h_{20} = ROLL WHEEL MOMENTUM AT COAST INCEPTION

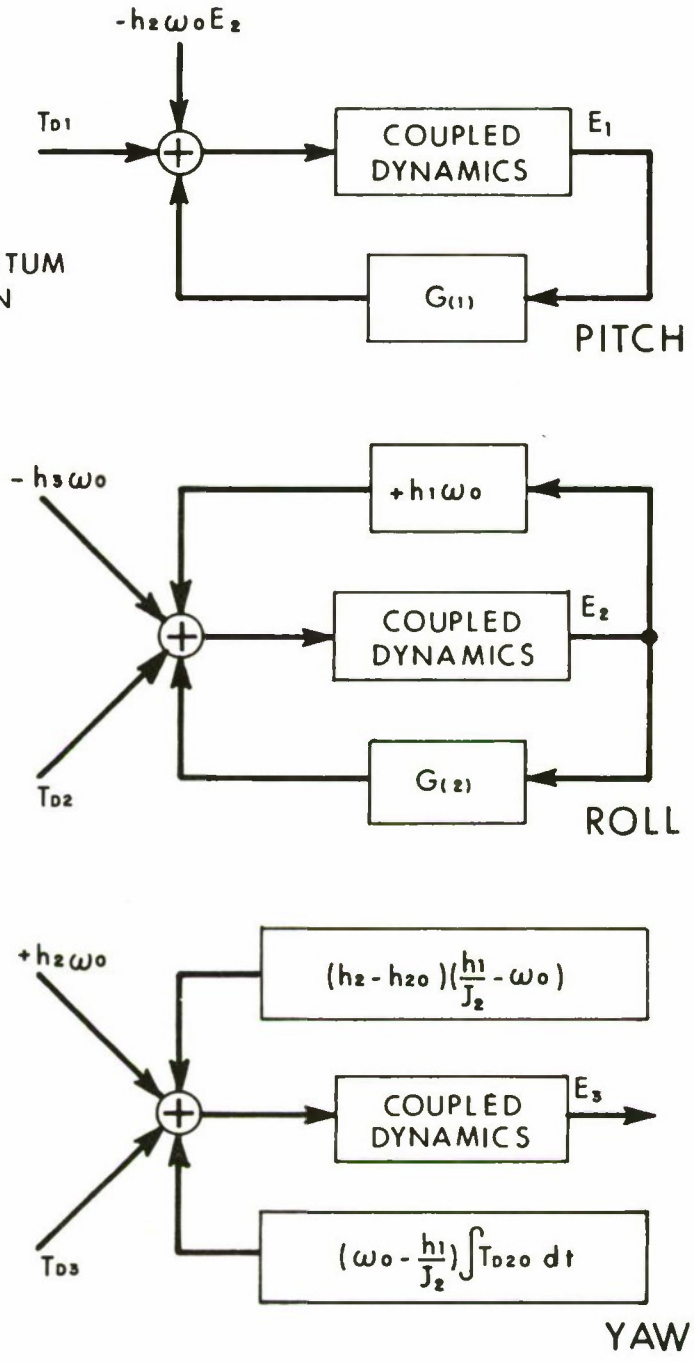

Fig. 6. Fully compensated axial torques during the coast period.

3. INERTIAL SYSTEM

It is proposed that the inertial system, in either of its two basic configurations, form the normal or operational mode of the attitude control system. The "backup mode" described earlier will be used only in the event of a catastrophic failure in the inertial unit.

3.1 Inertial Unit

When considering an inertial system with a projected life of 5 to 7 years, the reliability of the gyro instrument becomes the dominant question. Gyros have not, as yet, been applied to extended missions of this type in any quantity. Consequently, end-of-life failure mechanisms have not, in general, been established. While theoretical MTBF is quoted in the millions of hours, established MTBF based on actual performance is, for obvious reasons, an order of magnitude less, and is in terms of instrument hours. If gyros are to have any credence for a mission such as this, considerable redundancy will be required. It is therefore proposed that the inertial unit be based on the configuration suggested by Gilmore and McKern of CSDL in a 1970 AIAA paper.[3] In this arrangement geometric redundancy is achieved by using a non-orthogonal mounting configuration in which instrument input axes are oriented to correspond to the array of normals to the faces of a dodecahedron. This is shown in Fig. 7.

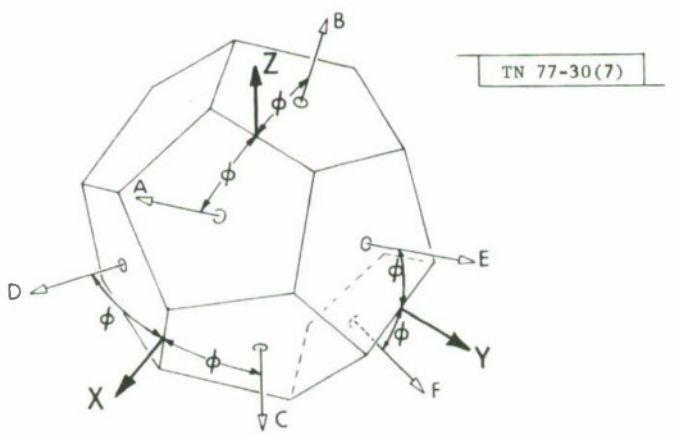

Fig. 7. Gyro axes with respect to a regular dodecahedron.

This arrangement yields a unique symmetry in which all instrument 1A's are at a spherical angle of 2ϕ from each other.

$$\phi = 31^\circ\ 48'\ 2.8''$$

The matrix relating the gyro axes and the vehicle principal axes is shown below.

$$\begin{bmatrix} \omega_A \\ \omega_B \\ \omega_C \\ \omega_D \\ \omega_E \\ \omega_F \end{bmatrix} = \begin{bmatrix} \sin\phi & 0 & \cos\phi \\ -\sin\phi & 0 & \cos\phi \\ \cos\phi & \sin\phi & 0 \\ \cos\phi & -\sin\phi & 0 \\ 0 & \cos\phi & \sin\phi \\ 0 & \cos\phi & -\sin\phi \end{bmatrix} \begin{bmatrix} \omega_X \\ \omega_Y \\ \omega_Z \end{bmatrix} \tag{27}$$

It is clear from this relationship that any three gyros are able to supply rate information about all three vehicle axes. It is proposed, therefore, that six SDF gyros, each with an independent set of electronics, be arranged in the hexad shown in Fig. 2. The selection of the gyro instrument is difficult, however, if we ignore for the present the TGG and the ESG, both of which show great promise, the most mature and documented inertial grade gyro available is the Northrop G1-K7G. This has a theoretical MTBF of 3×10^6 hrs, and an established instrument-hours MTBF of 3.4×10^5 hrs (39 yrs). If we use the established MTBF and a projected system life of 61,320 hrs (7 yrs) the "all-live" hexad reliability equation gives us the probability of system survival. (4)

$$R = +20e^{-3\lambda t} - 45e^{-4\lambda t} + 36e^{-5\lambda t} - 10e^{-6\lambda t} \tag{28}$$

$$\lambda t = \text{system life/gyro MTBF} = 0.18$$

$$R = 0.99122$$

This shows a greater than 99% chance of system survival over a 7-yr period. Survival is defined as any three instruments in operation. Furthermore, the above reliability equation assumes all six gyros are operating, if three are closed down until a failure occurs in one of the three operational instruments, then reliability is increased.

3.2 Inertial Sensor (1)

It is proposed that the following configuration be the normal day-day sensing system. It is felt that this configuration will cope adequately with a high gyro drift rate, and providing the updating algorithm is carefully chosen, will survive an optical sensor wipeout.

$\dot{\phi}_{Dj}$ is a nonlinear combination of three drift rates, and consequently has a greater variance than any single instrument. However, with the rates we are concerned with this is not significant.

The equations of motion for this system are given below (for the update loops closed).

$$(K_1 + B_1 \int dt)\ (E_1 + n - E_{10}) + \dot{E}_1 + \dot{\phi}_{D1} = \dot{E}_{10}$$

$$(K_2 + B_2 \int dt)\ (E_2 + n - E_{20}) + \dot{E}_2 - \omega_o E_3 + \omega_o E_{3o} + \dot{\phi}_{D2} = \dot{E}_{20}$$

$$(K_3 + B_3 \int dt)\ (E_3 + n - E_{3o}) + \dot{E}_3 + \omega_o E_2 - \omega_o E_{2o} + \dot{\phi}_{D3} = \dot{E}_{3o}$$

Solving these equations is straightforward if somewhat laborious; the results are shown below.

$$E_{10} = E_1 + \frac{(K_1 P + B_1)n}{\Delta 1(P)} + \frac{P^2 \phi_{D1}}{\Delta 1(P)}$$

$$\Delta 1(P) = P^2 + PK_1 + B_1$$

$$E_{20} = E_2 + \frac{[KP^3 + (K_2K_3+B_2+\omega_o K_3)\ P^2 + (K_2B_3+B_2K_3+\omega_o B_3)\ P + B_2B_3]\ n}{\Delta_{23(P)}}$$

$$+ \frac{[P^4 + K_3P^3 + B_3P^2]\ \phi_{D2} + \omega_o P^3 \phi_{D3}}{\Delta_{23(P)}}$$

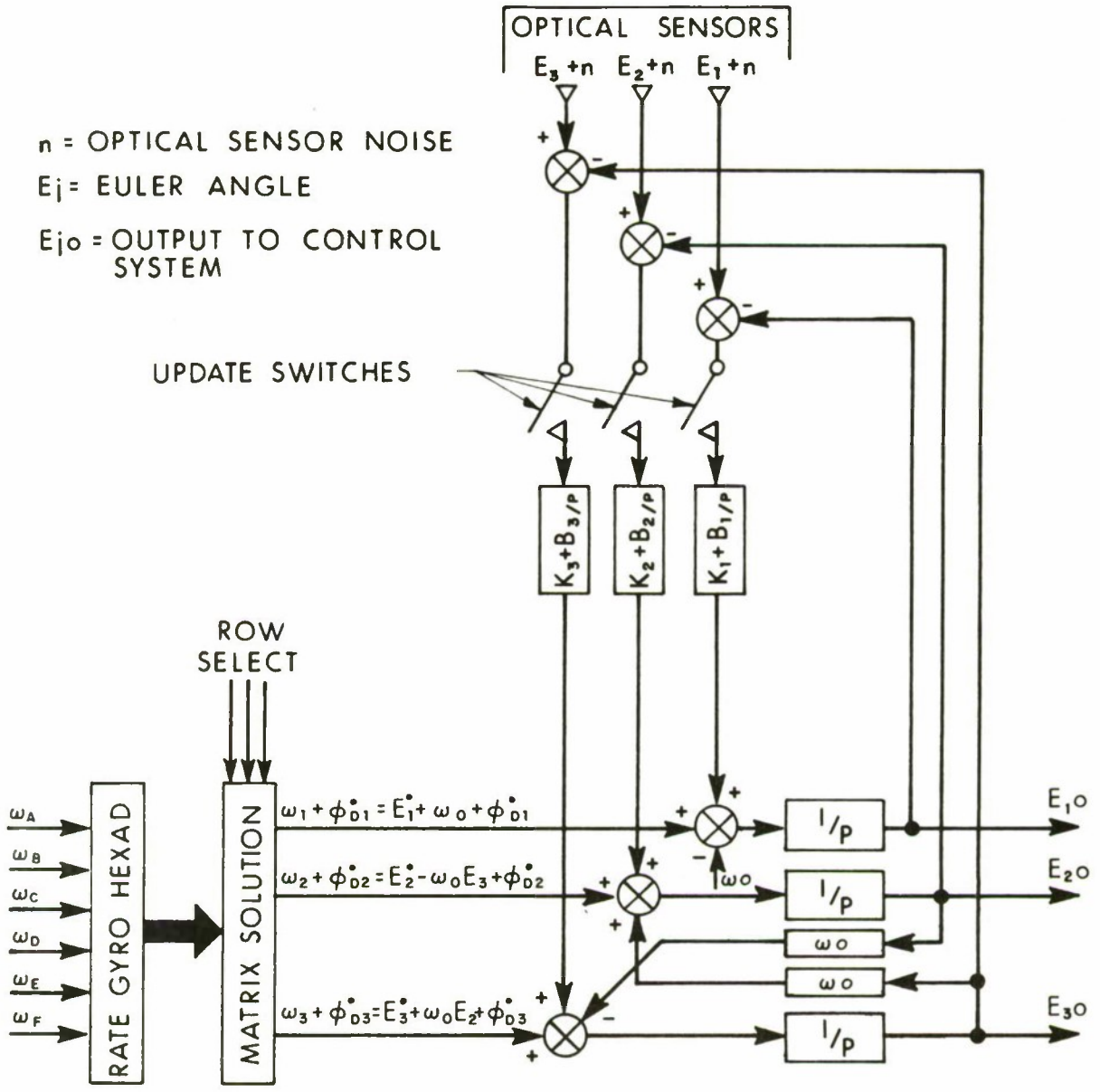

Fig. 8. Inertial system (1).

$$E_{30} = E_3 + \frac{[K_3P^3 + (K_2K_3+B_3-\omega_oK_2)\ P^2 + (K_2B_2+K_2B_3-\omega_oB_2)\ P + B_2B_3]\ n}{\Delta_{23(P)}}$$

$$+ \frac{[P^4 + K_2P^3 + B_2P^2]\ \phi_{D3} - \omega_oP^3\phi_{D2}}{\Delta_{23(P)}}$$

$$\Delta_{23(P)} = [P^4 + (K_2+K_3)\ P^3 + (B_3+B_2+K_2K_3+\omega_o^2)\ P^2 + (K_2K_3+B_2K_3)\ P + B_2B_3]$$

Notice that the system is self erecting in that in the absence of optical sensor noise and gyro drift terms, the error integrator output is equal to the euler angle. Notice also that gyro drift rate ($\dot{\phi}_{Dj}$) is not present at the integrator output, indicating that gyro drift rate will not produce vehicle attitude errors, derivatives of drift rate will. However, the magnitude of rate derivative terms is likely to be very small. A further point of interest is that the optical sensor noise term (n) will be operated on by a low-pass filter before appearing at the error integrator output. It seems clear that by suitable choice of loop constant (K&B) the control system can be effectively insulated from sensor noise during the update period.

The update algorithm is vital to the success of this system and will be discussed in a later section. It is not unreasonable to expect, however, that the update loop will be open most of the time.

3.3 Inertial Sensor (2)

Inertial system (1) discussed in 3.2 suffers from one slight disadvantage. If the optical sensors are indeed measuring the true Euler angles, then the system will self erect. However, the yaw error is derived from the sun elevation sensor based on a knowledge of the orbit parameters and the on-board solutions of several nonlinear equations. As a check on this fairly complex procedure it would be convenient to have available a second method of measuring yaw. Gyrocompassing supplies this method providing the composite drift

rate associated with the roll channel body rate measurement is $\bar{<}$ 0.02°/hr. It is suggested therefore that gyrocompassing form an alternate method of using the rate information produced by the gyro hexad. The method of connection is shown in Fig. 9.

When comparing this configuration with inertial system (1) described in Section 3.2, there are clearly three major changes. The most obvious is the fact that both yaw and roll are erected by the roll optical sensor. This is inherent to orbital gyro-compassing, in which the roll sensor provides the necessary vertical reference for yaw. Secondly the integrator is no longer present in the roll optical sensor channel. This is because in the orbital gyro-compass configuration the integrator is no longer beneficial and does not cancel drift rate.[5] The major yaw error source is the gyro drift rate associated with the roll body rate measurement. With the hexad configuration the drift term will depend upon which three gyros are in use. When using inertial system (1) this is not important because the roll optical sensor integrator will absorb whatever drift term is produced; however, with the gyro-compass configuration (inertial system (2)) this is not true. The drift term must either be known and programmed in from the ground, or we must trust the yaw optical sensor, in which case we simply disconnect the input of the roll optical sensor integrator when transferring from inertial system (1). This situation is unlikely to produce any difficulty, in order to cover 360° in pitch we will have four separate sun elevation sensors, in extremis it would be a trivial matter to derive roll gyro drift rate bias from any of these.

The equations of motion for inertial system (2) (Fig. 9) are shown below (update mode).

To make the point regarding drift bias cancellation quite clear, we will assume in the following analysis that all three channels include an integral plus proportional network in series with the optical sensor. That is, referring to Fig. 9, the box containing K_2 only will be assumed to contain $K_2 + B_2 \int dt$.

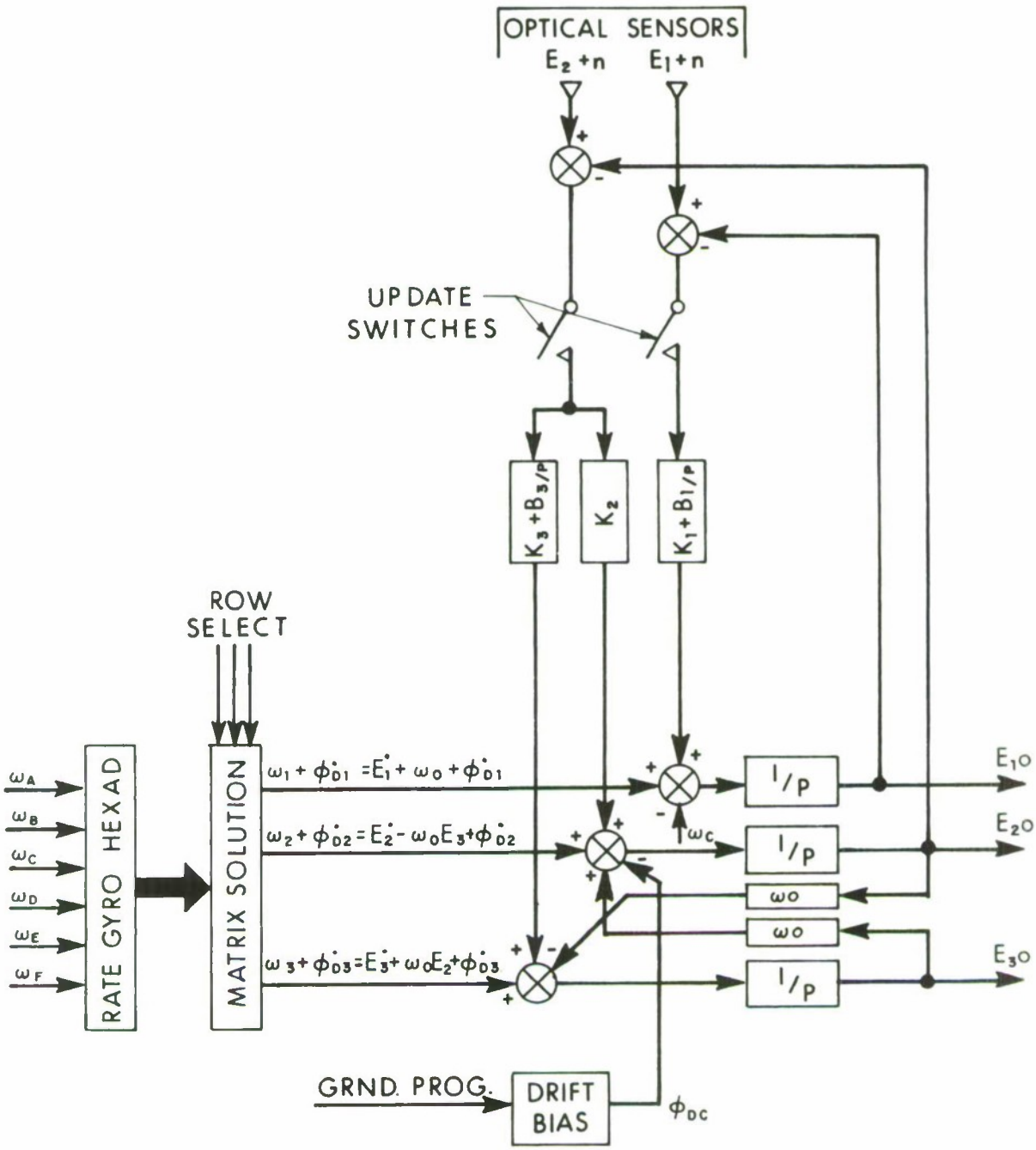

Fig. 9. Inertial system (2) (Gyro-compass).

$$(K_1+B_1 \int dt)\ (E_1+n-E_{10}) + \dot{E}_1 + \dot{\phi}_{D1} = \dot{E}_{10}$$

$$(K_2+B_2 \int dt)\ (E_2+n-E_{20}) + \dot{E}_2 - \omega_o E_3 + \omega_o E_{30} + \dot{\phi}_{D2} - \dot{\phi}_{DC} = \dot{E}_{20}$$

$$(K_3+B_3 \int dt)\ (E_2+n-E_{20}) + \dot{E}_3 + \omega_o E_2 - \omega_o E_{20} + \dot{\phi}_{D3} = \dot{E}_{30}$$

Once again the solution of these equations is simple, if incredibly laborious. The pitch equation is identical with inertial system (1), therefore we will ignore it.

$$E_{20} = E_2 + \frac{[K_2P^2 + (B_2+\omega_o K_2)\ P + \omega_o B_3]\ n}{\Delta'_{(P)}} + \frac{\omega_o P^2 \phi_{D3} + P^3(\phi_{D2}-\phi_{DC})}{\Delta'_{(P)}}$$

$$E_{30} = E_3 + \frac{[K_3P^2 + (B_3-\omega_o K_2)\ P - \omega_o B_2]\ n}{\Delta'_{(P)}} + \frac{[P^3 + K_2P^2 + B_2P]\ \phi_{D3}}{\Delta'_{(P)}}$$

$$+ \frac{[P^2(K_3+\omega_o) + B_3P]\ (\phi_{DC}-\phi_{D2})}{\Delta'_{(P)}}$$

$$\Delta'_{(P)} = P^3 + K_2P^2 + (B_2+K_3\omega_o+\omega_o^2)\ P + \omega_o B_3$$

Notice that despite the lack of an optical yaw sensor the system is self erecting, such that in the absence of optical sensor noise and gyro drift terms the error integrator outputs are equal to the Euler angles. Notice also that the optical sensor noise term (n) is filtered before appearing on the error integrator output. As in the case of inertial system (1), with proper selection of loop constants (K&B) the control system would receive a very quiet error signal. The behavior of the composite gyro drift term is interesting, in order to make this clear let us assume that the cancelling term $\phi_{DC} = 0$. In the case of the roll channel both roll and yaw drift terms are present but in a rate derivative form, therefore drift rate does not contribute in any way to roll error.

In the case of yaw, if we let the rate derivative terms approach zero, and solve for the yaw end value, ignoring sensor noise (n).

$$E_{30(S.S.)} = E_3 + \frac{B_2}{B_3} \cdot \frac{\dot{\phi}_{D3}}{\omega_o} - \frac{\dot{\phi}_{D2}}{\omega_o}$$

In this case the optical sensor integrators have not cancelled the drift rate term as they did for pitch and roll. In fact they have increased the variance. It seems that we can only benefit by letting $\beta_2 = 0$, that is by removing the optical sensor integrator in the roll channel, as shown in Fig. 9. If we therefore let

$$\phi_{D2} = \phi_{DC}$$

$$\beta_2 = 0 \quad .$$

The expressions for the error integrator outputs wll be as shown below. Assuming drift rate derivatives → 0,

$$E_{20} = E_2 + \frac{[K_2P^2 + \omega_o K_2 P + \omega_o B_3]\ n}{\Delta_{(P)}}$$

$$E_{30} = E_3 + \frac{[K_3P^2 + (B_3 - \omega_o K_2)P]\ n}{\Delta_{(P)}}$$

$$\Delta_{(P)} = P^3 + K_2P + \omega_o(K_3+\omega_o)\ P + \omega_o B_3$$

3.4 The Inter-Update Period

In order to investigate the operation of the inertial systems between updates, that is when the optical sensors are disconnected. We need only consider inertial system (1).

As we are considering the inter-update period, then it is not unreasonable to expect the composite gyro drift terms to be nulled by the integrators in the optical sensor path. In this case the linearized equations of motion reduce to:

$$\int \dot{E}_1 \, dt = E_{10}$$

$$\dot{E}_2 - \omega_o E_3 + \omega_o E_{30} = \dot{E}_{20}$$

$$\dot{E}_3 + \omega_o E_2 - \omega_o E_{20} = \dot{E}_{30}$$

Solving for the error integrator outputs,

$$E_{10} = E_1$$

$$E_{20} = E_2$$

$$E_{30} = E_3$$

This highly desirable result is brought about by reproducing the kinematic cross coupling within the inertial system configuration.

3.5 Gyro System Update

The justification for the highly redundant gyro system proposed is the assumption that the satellite will be attacked in a manner which will damage the optical sensors but not the gyro system, which is assumed to be adequately shielded by the satellite body. If this scenario is accepted then the gyro system must be erected and operational at all times, and it must be shown, as I think it has been, that the gyro system has a high probability of remaining operational for the projected life of the satellite. Furthermore, any method used to update the gyros from the optical sensors must be one which has a very low probability of de-erecting the gyro system in the event that the optical sensors are destroyed. Referring to Fig. 8, the update switches open or close the connection between the optical sensors and the gyro system. It is intended that this connection will be made when updating is required and broken only when updating is deemed to be complete.

The update period, when the connection is made, is likely to be a very small percentage of the total time. A high quality inertial grade gyro such as the TGG or G1-K7G, properly compensated, can be expected to remain erected within the pointing tolerance for several months when operated in a zero acceleration environment. Whereas updating, when required, will occupy a few minutes. Furthermore, the method of drift correction suggested for Inertial System (1) is inherently error free. So infrequent is updating likely to be that consideration must be given to operating the update switches manually by ground command.

However, other considerations may indicate the desirability of an automatic system which is therefore discussed below.

Update Algorithm

Any automatic method of operating the update switches must make the following decisions.

1. Is an update required?
2. Is an update complete?
3. Is the optical sensor output valid?

The algorithm will not attempt to judge gyro validity. This is a quite separate problem which can also be automated to some limited extent; however, in the interests of simplicity and reliability, it is recommended that this function be performed by multi-sensor observation followed by appropriate action by ground control.

Condition (1)

In general a gyro update will be required whenever the optical sensor error angle no longer equals the output of the gyro system error integrator. However, optical sensor noise together with gyro short term random drift rates will insure that this is always true. Fortunately our concern is with relatively long term (several hours) changes in gyro drift rate bias. It will therefore be possible to average this difference over some long period,

$$\frac{1}{T} \sum_{t=o}^{t=T} (E_{os}-E_{io})t \overline{>} |0.1°| \qquad (1)$$

T = programmable averaging period

E_{os} = Optical Sensor Output

E_{io} = Gyro Error Integrator Output

Condition (2)

Condition (2) follows directly from (1). If the optical sensor output error angle is equal to the gyro system error integrator output, then irrespective of body rates, the gyro is erected.

$$\frac{1}{T} \sum_{t=o}^{t=T} (E_{os}-E_{io})t \overline{<} |0.01°| \qquad (2)$$

Condition (3)

This condition overrides the previous two, and is the most difficult to mechanize. It does, however, divide into two distinct areas, the gross operation of the optical sensor and the characteristics of the output signal.

The gross operation is simply the measurement of the various characteristic waveforms, voltages and currents, etc., which would characterize a normally operating and appropriately stimulated optical sensor. The output characteristic measurement would be an attempt to detect gross changes in the noise envelope by measurement of threshold crossing rates. This would involve the establishment of two symmetrical amplitude thresholds centered about the average sensor output. The mean rate of threshold crossing would be measured on a continuous basis and compared with stored programmable norms. If we assume a Gaussian distribution for the noise this method would be very sensitive to changes in RMS noise level. It would also detect, as noise, random departures from the mean level due to other sensor malfunctions. This method would assume that the change of sensor error would be very small during the averaging time. During normal operation this would be true.

$$H_T = \frac{1}{T} \sum_{t=o}^{t=T} (E_{os})t \pm K_H$$

$$H_L = \frac{1}{T} \sum_{t=o}^{t=T} (E_{os})t \pm K_L$$

$$\text{Mean Expected Time} = \frac{1}{\beta} \exp - \frac{K_{(HL)}}{2\psi_o}$$

H_T, H_L = absolute amplitude of high and low threshold respectively

K_H, K_L = programmable high and low thresholds

β = system bandwidth

The algorithm conditions are summarized below.

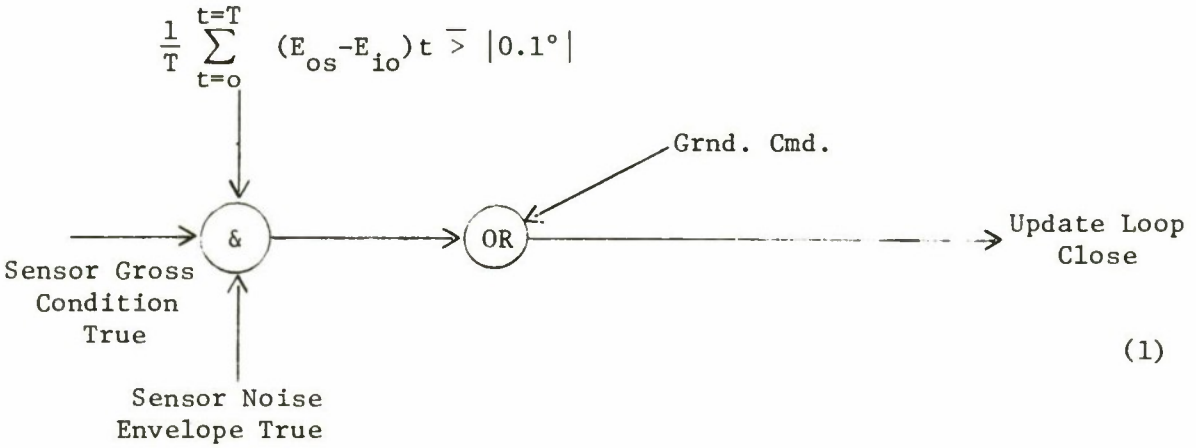

(1)

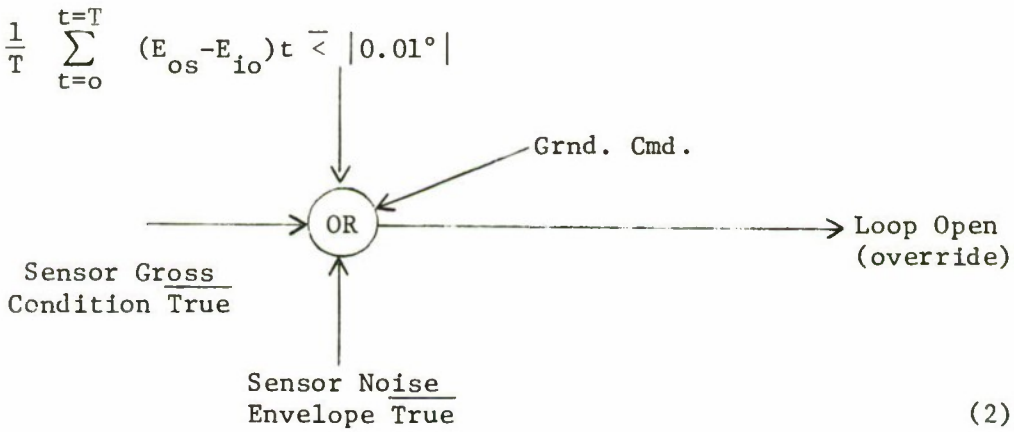

(2)

The foregoing has outlined the system configuration and analyzed in a general way the three major attitude sensing arrangements. The gyro instrument tentatively suggested for the HEXAD, the Northrop G1-K7G, is probably the most mature and documented inertial grade instrument presently available, and as such is able to provide hard reliability data. However, the two axis ESG presently under development by Honeywell and Autonetics has a theoretical MTBF limited largely by the electronics. This clearly suggests a reliability potential considerably in excess of present instruments. The ESG must therefore be considered a very strong contender for the gyro system instrument.

```
FILE: COMP4    FORTRAN  A    6/16/77 15:33    M.I.T. LINCOLN LABORATORY

C  WB SMITH   TEST NORDSIECK INTEGRATION ROUTINE
C
C     MAIN PROGRAM FOR DYNAMIC SIMULATION ROUTINE.  INITIALIZATION AND
C     SPECIFICATION OF INTEGRAL PARAMETERS IS PERFORMED.
C
      IMPLICIT REAL*8 (A-H,O-Z)
      COMMON/ADAMS/DYDT(180,15),DYDTO(180),NPREDT,NCORFT,NEQ,NH
     1 ,INTEMX,ITYPE
      COMMON/INCON/HC,HMX,HMN,EPS,T,N,M,L1
      COMMON/SIINT/VO(180),TO,TSTOP
      COMMON/NMSTRT/AO(180),BO(180),CO(180),DO(180),EEO(180),HSAVE,
     1 BOTH,LBOTH,NSIGN,FO(180)
      COMMON /TORQ/ID1,ID2,TD3
C
C
      ITYPE=1
C
C     NUMBER OF D.E. EQUATIONS
C
      M=11
      N=11
      L1=0
      HC=10.D0
C
C     MINIMUM STEP SIZE
C
      HMN=1.D-4
C
C     T INITIAL
C
      TO=0.D0
C
C     T FINAL
C
      TSTOP=24.0D0*3600.D0
      NSIGN=1
C
C     MAXIMUM STEP SIZE
C
      HMX=100.D0
      EPS=1.D-8
C
C     INITIALIZATION OF INTEGRALS
C
      DO 100 I=1,N
100   VO(I)=0.D0
      VO(7)=-1000.0D0/28.D0
C
C     TORQUES ARE ENTERED
C
      WRITE (2,1)
1     FORMAT (' INPUT TORQS IN MICRO-FT.LBS.')
      READ (2,*) TD1,TD2,TD3
      TL1=TD1*1.D-6
      TL2=TD2*1.D-6
```

```
      TD3=TD3*1.D-6
C
C     CALL TO INTEGRATION ROUTINE
C
      CALL NUMINT
      END
C
C
C
C     COMPUTATION OF DERIVATIVES IS PERFORMED IN THE FUNCTION FN
C
      DOUBLE PRECISION FUNCTION FN(K,J,S)
      IMPLICIT REAL*8 (A-H,O-Z)
      REAL*8 WO/72.722051217D-6/,J1/2800.D0/,J2/2800.D0/,J3/2800.D0/
      REAL*8 TD20/49.57D-6/
C     REAL*8 K1/280.D0/,K2/280.D0/,K3/280.D0/
      REAL*8 K1/280.D0/,K2/0.D0/,K3/0.D0/
C     REAL*8 B1/28.D0/,B2/28.D0/,B3/28.D0/
      REAL*8 B1/28.D0/,B2/0.D0/,B3/0.D0/
      REAL*8 KT/0.0D0/,K11/1.D0/,K22/1.D0/,K33/1.D0/
      REAL*8 K4/0.D0/,K5/1.D0/,K6/1.D0/
      COMMON/OUTPUT/K1OUT,K2OUT,V(180,4),F(180,3)
      COMMON/STINT/V0(180),T0,TSTOP
      COMMON /TORQ/TD1,TD2,TD3
      COMMON /XTERMS/H1,H2,H3
      COMMON/INCON/HC,HMX,HMN,EPS,T,N,M,L1
C
C     THE VARIABLE K SELECTS THE DERIVATIVE TO BE COMPUTED
C
      GO TO (10,20,30,40,50,60,70,80,90,100,110),K
10    CONTINUE
C
C     THE VALUES OF H1, H2, AND H3 ARE COMPUTED
C
      H1=-K1*K11*V(1,J)-B1*K11*V(7,J)
C     H2=-K2*K22*V(2,J)-B2*K22*V(8,J)
C     H3=-K33*(K3*V(3,J)+B3*V(9,J))-KT*V(10,J)/J2
C     H1=0.D0
      H2=0.D0
      H3=0.D0
C
C     E1 IS COMPUTED FROM DE1/DT
C
      FN=V(4,J)
      GO TO 600
C
C     E2 IS COMPUTED FROM DE2/DT
C
20    FN=V(5,J)
      GO TO 600
C
C     E3 IS COMPUTED FROM DE3/DT
C
30    FN=V(6,J)
      GO TO 600
```

```
C
C       DF1/D1 IS COMPUTED
C
40      FN=(-H3*V(5,J)+H2*(W0*(V(2,J)*K6+V(3,J))+V(6,J))
     *  +TD1*DSIN(W0*T)-V(4,J)*K1-V(1,J)*B1)/J1
        GO TO 600
C
C       DF2/DT IS COMPUTED
C
50      FN=(WC*((J2-J1+J3)*V(6,J)-(J1-J3)*W0*V(2,J))
     *  -H1*(V(6,J)+W0*V(2,J)*K6)+H3*(V(4,J)+W0*K5)
     *  +TD2*DSIN(WC*(T))-V(5,J)*K2-V(2,J)*B2)/J2
C    *  +TL2-V(5,J)*K2-V(2,J)*B2)/J2
        GO TO 600
C
C       DF3/DT IS COMPUTED
C
60      FN=(-W0*((J2-J1+J3)*V(5,J)-(J2-J1)*W0*V(3,J))
     *  -H2*(V(4,J)+WC*K5)+H1*(V(5,J)-W0*V(3,J))
C    *  +W0*(V(11,J)+H2)-H1*(V(11,J)+H2)/J2
     *  +TD3*DCOS(W0*(T))-V(6,J)*K3*K4-V(3,J)*B3*K4)/J3
C    *  +TD3-V(6,J)*K3*K4-V(3,J)*B3*K4)/J3
        GO TO 600
C
C       THE INTEGRAL OF E1 IS COMPUTED
C
70      FN=V(1,J)
        GO TO 600
C
C       THE INTEGRAL OF E2 IS COMPUTED
C
80      FN=V(2,J)
        GO TO 600
C
C       THE INTEGRAL OF E3 IS COMPUTED
C
90      FN=V(3,J)
        GO TO 600
C
C       THE INTEGRAL OF H1*H2 IS COMPUTED
C
100     FN=H1*H2
        GO TO 600
C
C       THE INTEGRAL OF TD20 IS COMPUTED
C
110     CONTINUE
C       FN=TD20*DSIN(W0*(T))
        FN=TD20
C       FN=TD2
600     CONTINUE
C       WRITE (2,*) K,J,V(K,J)
        RETURN
        END
C
```

```
FILE: COMP4    FORTRAN  A    6/16/77 15:33    M.I.T. LINCOLN LABORATORY


C
C
C     THE OUTPUT FILE IS CREATED BY THE SUBROUTINE GIVOUT
C
      SUBROUTINE GIVOUT
      IMPLICIT REAL*8 (A-H,O-Z)
      INTEGER ICNT/0/
      REAL*8 W0/72.722041217D-6/
      COMMON/INCON/HC,HMX,HMN,EPS,T,N,M,L1
      COMMON/OUTPUT/K1,K2,V(180,4),F(180,3)
      COMMON/STINT/VC(180),TO,TSTOP
      COMMON /XTERMS/H1,H2,H3
      COMMON /TORQ/TD1,TD2,TD3
      ICNT=ICNT+1
      IF (ICNT.GT.1000) GO TO 100
      TORQ1=TD1
      TORQ2=TD2*DSIN(W0*(T))
      TORQ3=TD3*DCOS(W0*(T))
C
C     DATA IS WRITTEN TO OUTPUT FILE
C
      WRITE (10,2) T,(V(I,3),I=1,6),TORQ1,TORQ2,TORQ3
2     FORMAT (10A8)
C     IF (60*(ICNT/60).EQ.ICNT) WRITE (2,*) ICNT,T
      WRITE (2,*) ICNT,T
C     WRITE (2,3) T,(V(I,3),I=1,10)
C     WRITE (2,4) H1,H2,H3
4     FORMAT (1X,3(1X,F10.3))
3     FORMAT (1X,F10.2,10(1X,F10.4))
1     FORMAT (8(1X,D15.4))
      RETURN
100   WRITE (2,1) T,HC,(V(I,3),I=1,10)
      STOP
      END
```

References

1. N. R. Trudeau, "Yaw Error Measurement Using Sun Elevation Sensor," private communication (15 March 1977).

2. J. R. Vernau, "LES-10 Inertial ACS," private communication (19 July 1976).

3. G. P. Gilmore and R. A. McKern, "A Redundant Strapdown Inertial Reference Unit (SIRU)," CSD 9, No. 1 (January 1972).

4. SURVSATCOM Attitude Reference Navigation System (ARNS) Configuration Study, Northrop Corporation Electronics Division, Precision Products Department.

5. J. R. Vernau, "Orbital Gyrocompassing," private communication (29 September 1976).

ACKNOWLEDGEMENT

Geoffrey T. Flanders was responsible for all the computer programming associated with this note. This comprised the machine solution of the system equations of motion (24), (25), (26) for a variety of body torques and initial conditions, and the production of computer generated system responses. It was from these results that Figs. 2, 3, 4 and 5 were derived.

REPORT DOCUMENTATION PAGE		READ INSTRUCTIONS BEFORE COMPLETING FORM
1. REPORT NUMBER ESD-TR-77-173	2. GOVT ACCESSION NO.	3. RECIPIENT'S CATALOG NUMBER
4. TITLE *(and Subtitle)* An Attitude Control System for a Large Geosynchronous Earth-Pointing Satellite		5. TYPE OF REPORT & PERIOD COVERED Technical Note 6. PERFORMING ORG. REPORT NUMBER Technical Note 1977-30
7. AUTHOR*(s)* Joseph R. Vernau		8. CONTRACT OR GRANT NUMBER*(s)* F19628-76-C-0002
9. PERFORMING ORGANIZATION NAME AND ADDRESS Lincoln Laboratory, M.I.T. P.O. Box 73 Lexington, MA 02173		10. PROGRAM ELEMENT, PROJECT, TASK AREA & WORK UNIT NUMBERS Program Element No. 63431F Project No. 1227
11. CONTROLLING OFFICE NAME AND ADDRESS Air Force Systems Command, USAF Andrews AFB Washington, DC 20331		12. REPORT DATE 5 July 1977 13. NUMBER OF PAGES 48
14. MONITORING AGENCY NAME & ADDRESS *(if different from Controlling Office)* Electronic Systems Division Hanscom AFB Bedford, MA 01731		15. SECURITY CLASS. *(of this report)* Unclassified 15a. DECLASSIFICATION DOWNGRADING SCHEDULE

16. DISTRIBUTION STATEMENT *(of this Report)*

Approved for public release; distribution unlimited.

17. DISTRIBUTION STATEMENT *(of the abstract entered in Block 20, if different from Report)*

18. SUPPLEMENTARY NOTES

None

19. KEY WORDS *(Continue on reverse side if necessary and identify by block number)*

satellite systems	inertial system	optical attitude sensors
attitude control system	torque environment	attitude sensing

20. ABSTRACT *(Continue on reverse side if necessary and identify by block number)*

The proposed attitude control system addresses three principal problem areas:

(1) Operation within a high disturbance torque environment,
(2) The preservation of vehicle attitude in the event that the optical attitude sensors are destroyed by external means, and
(3) System operational longevity.